CFD Modeling and Simulation in Materials Processing 2016
Edited by: Laurentiu Nastac, Lifeng Zhang, Brian G. Thomas, Miaoyong Zhu, Andreas Ludwig, Adrian S. Sabau, Koulis Pericleous, and Hervé Combeau
TMS (The Minerals, Metals & Materials Society), 2016

SIMULATION OF HEAT TRANSFER IN SLAB CONTINUOUS CASTING MOLD AND NEW FORMATION MECHANISM OF SHELL HOT SPOTS

Zhaozhen Cai, Miaoyong Zhu

School of Materials and Metallurgy, Northeastern University, Shenyang, 110819, China

Keywords: Slab continuous casting, Mold, Heat transfer, Air gap, Mold flux film, Hot spots

Abstract

A mathematical model of simulating the heat transfer behavior of carbon steel solidifying in slab continuous casting mold was developed coupled with heat transfer media dynamic distribution behavior in shell/mold gap, such as liquid flux, solid flux, air gap, as well as mold/solid flux interfacial contact thermal resistance. The evolution characteristics of the distributions of mold flux, air gap formation, as well as the shell temperature field of carbon steel solidifying in a slab mold were described. Based on these, a new mechanism of shell hot spots formation in slab mold was proposed. The formation for shell wide face off-corner hot spot at mold upper and middle parts results from the thick mold flux film filling in shell/mold gap, while the lower part results from the thick air gap formation, and that of the narrow face just results from the thick mold flux film filling in the gap.

Introduction

Continuous casting is the most primary way of producing steel currently owing to its inherent advantages over ingot casting such as low cost, energy saving, flexibility of operation, and high quality cast product [1], and over 90% of steel in the world today is produced by this process. However, there are also numerous of defects often occurring in slabs surface and subsurface in practical continuous casting in steel plants, which are directly related to the thermal and mechanical behaviors of initial solidified shell in mold. Among these defects, the off-corner surface depressions and subsurface cracks, which results from the formation of hot spots on initial solidifying shell surface in mold, appear rather commonly. [2-4] Intending to reduce the occurrence rate of the defects, several studies have been conducted to investigate the shell thermal behaviors and the mechanisms of hot spots formation in shell surface in continuous casting mold in past decades by numerical simulation. [5-12]

Brimacombe et al. [5] studied the shell temperature evolution in a slab continuous casting mold by using a mathematical model coupled with the process of air gap formation in shell/mold gap with the shell deformation, and the formation mechanism of shell off-corner hot spots that resulted from the air gap formation in the regions was proposed. Kristiansson [6] also simulated the shell temperature filed in a billet mold by a two dimensional thermo-mechanical coupled model, and the hot spots formation cause was regarded as the reduced heat transfer in shell off-corners due to the air gap formation. Wang et al. [7, 8] studied shell thermo-mechanical behaviors in billet mold by using a gap-dependent heat transfer model to calculate the heat flux through the air gap, and the shell hot spots formation was also considered that they were resulted from the air gap formation. These previous works have a common point that the investigations on shell thermal behavior in mold did not consider the influence of mold flux film on the heat transfer

L. Nastac et al. (Eds.), *CFD Modeling and Simulation in Materials Processing 2016*

that the shell/mold gap just filled in the air gap. However, in practical continuous casting, the mold flux film in the gap has a great significant effect on shell heat transfer. [13-15] In order to consider the influence, Kim et al. [9] and Han et al. [10] studied shell temperature evolutions in beam blank and slab molds by developing finite element models with assuming uniform mold flux film of 100μm in shell/mold gap. Thomas et al. [11, 12] studied the shell temperature fields in slab and billet molds by developing finite element models based on the variation thickness of mold flux film in shell/mold gap along mold height. Nevertheless, both of them did not consider the distribution characteristics of the flux film along mold circumference that it was assumed uniformly along the circumference. Accordingly, the formation of shell hot spot in mold also attributed to the air gap formation. However, the practical continuous casting and several studies showed that the mold flux film in the mold both along mold circumference and height were nonuniform and affected the air gap formation and shell heat transfer in mold greatly. [14, 16, 17]
In present work, a two dimensional transient heat transfer model of simulating the strand-mold system heat transfer behaviors of carbon steel solidifying in slab continuous casting mold was developed coupled with shell deformation, in which the heat transfer behaviors of shell/mold gap were described in detail with the considerations of the gap size evolution, mold flux film dynamic distribution and air gap formation in it. Based on these, the characteristics of the mold flux film dynamical distribution, air gap formation, as well as the shell temperature field and the growth of a carbon steel solidifying in slab mold in a plant were analyzed, and a new mechanism for shell hot spots formation in slab mold was proposed by analyzing the evolution characteristics of shell surface temperature and the thermal resistances of mold flux and air gap in the shell/mold gaps of the wide and narrow faces.

Model descriptions

In our previous study [18], to describe the heat transfer process of shell solidification in a continuous casting mold in detail, a two dimensional slice-travel transient thermo-mechanical coupled model of a quarter of a strand-mold system were developed, as shown in **Fig. 1**.

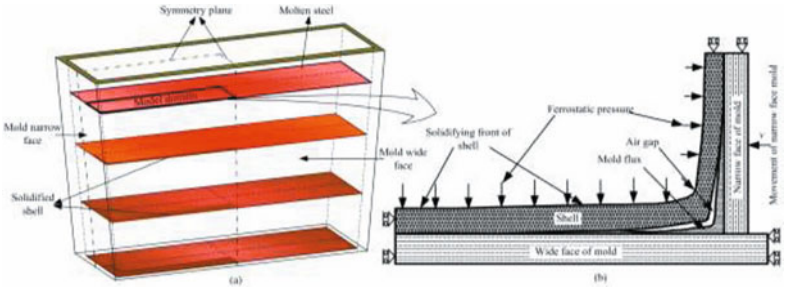

Fig. 1 Schematic of the shell thermo-mechanical simulation model for a slab mold: (a) the calculation domain, (b) transverse section of a slice

In this model, the shell heat transfer and stress evolution were predicted by a sequential coupling method. The heat transfers of strand and mold copper plate were governed by the two-dimensional transient heat transfer equation based on the strand surface and mold hot face heat transfer boundary conditions of the shell/mold gap heat flux obtained from the detailed

description of shell/mold gap heat transfer. The shell deformation and stress evolution were predicted by an Anand constitutive model [19, 20], and the mold copper plate deformation was neglected. The contact behavior between the shell and mold was set as rigid-to-flexible contact. The ferro-static pressure was loaded onto the shell solidification front using an algorithm that dynamically rejected the "liquid element" as the shell solidification proceeded.

For the description of the shell/mold gap heat transfer, the shell/mold gap was assumed to be fully filled by the mold flux film and air gap, and the area was not meshed. The gap size evolution was predicted by shell shrinkage and deformation within each time step as the shell moves down. The mold flux film in the gap was considered to consist only of liquid and solid flux, and the (liquid/solid) status was determined by both the shell surface temperature and its solidification temperature. The thickness of the film was determined by both the status of the mold flux and the shell/mold gap size. In accordance with practical continuous casting, the heat transfer of the shell/mold gap was divided into two modes according to the different heat transfer media used to fill it; specifically, the composition of mode I consisted of the liquid flux, the solid flux, and the mold/solid flux interfacial contact thermal resistance, and that of mode II consisted of the air gap, the solid flux, and the mold/solid flux interfacial contact thermal resistance. As an important part of the gap heat transfer [21, 22], the radiation heat transfers in the air gap and mold flux film were taken into account. The air gap formation, mold flux film distribution, and the corresponding thermal resistances around the mold circumference were calculated according to the mechanism of the same heat flux across the heat transfer medium layers based on the parameters of the shell surface and mold hot-face temperatures and the shell/mold gap size along mold circumference provided by the previous time-step of strand-mold thermo-mechanical behavior analyses. The more detailed calculation model was shown in our previous study [18].

Results and discussion

3.1 Mold flux film distribution and air gap formation in mold

Fig. 2 shows the predicted distribution characteristics of mold flux film in shell/mold gap around the shell off-corners at the distances of 100mm, 300mm, 500mm below meniscus and mold exit as the effect of above shell deformation characteristics. At the upper part of mold, the mold flux films both around shell wide and narrow faces decrease gradually from the corners to the midst. Nevertheless, the distributions are relatively uniform that the differences of the thicknesses between the corners and the midst are just 0.20mm and 0.32mm for the wide and narrow faces,

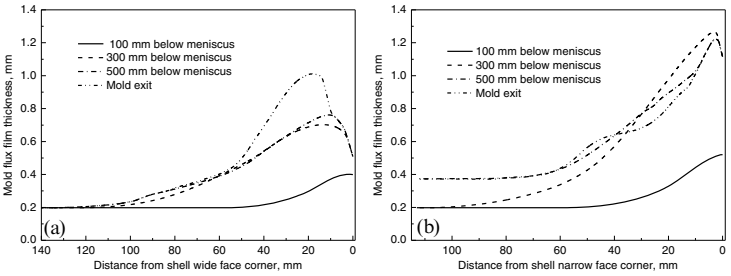

Fig. 2 Mold flux distribution around shell wide face corner (a) and narrow face corner (b)

respectively, when shell moves down to 100mm below meniscus. However, with the shell moving down continuously, the mold flux films completely solidify gradually from the corners to the midst, and thus the distributions show a trend that increase firstly and decrease then in the regions of 0–120mm and 0–70mm off the shell wide and narrow face corners respectively with the evolution of the shell/mold gap. The maximum differences of the thicknesses between the regions and the corresponding midst reach 0.81mm at mold exit and 1.07mm at 300mm below meniscus, respectively. It will greatly slow down the heat transfer of the off-corners.

Fig. 3 shows the predicted air gap distributions around the shell wide and narrow face corners. Under the casting conditions of the carbon steel, the air gap first forms in the shell corner at 160mm below meniscus and mainly concentrates in the regions of 0–20mm and 0–10mm off shell wide and narrow face corners, respectively. On the wide face due to lack of the compensation of mold wide face taper, the air gap grows continuously at mold upper and middle parts as the shell moves down, as shown in Fig. 3(a). When the shell moves down to the position of 550mm below meniscus, the air gap increases rather quickly. The maximum thickness of the air gap reaches 0.8mm at the corner.

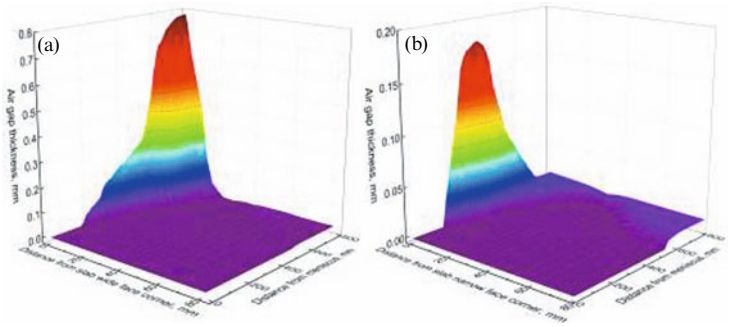

Fig. 3 Air gap distribution around shell wide face corner (a) and narrow face corner (b)

For shell narrow face, the air gap formation is quite different, as shown in Fig. 3(b). It mainly forms in the range of 160–450mm below meniscus, and is much thinner than that of wide face since the compensation of mold narrow face taper and more mold flux filling the gap restrain the formation. In the upper part of the mold, the air gap forms quickly and even exceeds that of the wide face. It reaches a maximum thickness of 0.17mm at 300mm below the meniscus, and then decreases sharply since the shell shrinkage slows down and the mold taper compensates. When shell moves down below 450mm from meniscus, the air gap becomes stable.

3.2 Shell surface temperature distribution

Fig.4 shows the surface temperature distributions of the solidifying shell near the corner along the height of mold. At the initial solidification stage, the shell surface temperature on wide face and narrow face is uniform. However, with the shell moving down, the heat transfers both around shell corner and off-corner slow down gradually since the thick mold flux film and air gap fill in the gap of these regions. When the shell moving down to 300mm below meniscus, the

hot spots form in the regions of 10–40mm both off shell wide and narrow face corners, and extend to the regions of 10–80mm and 15–60mm off the wide and narrow face corners when the shell moves down to mold exit, which the maximum temperature differences between the off-corners and the corresponding midst reach 120 ºC at mold exit and 129 ºC at 300mm below meniscus, respectively.

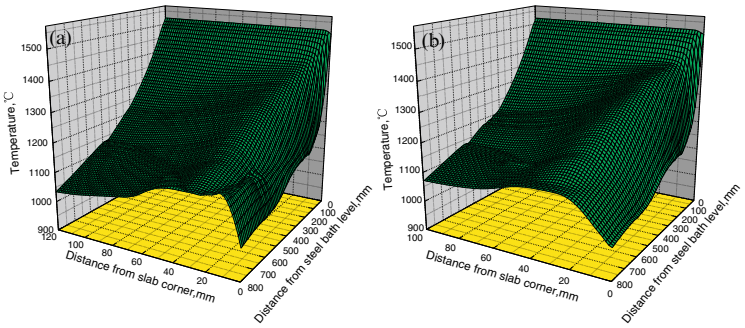

Fig.4 Shell surface temperature distribution at wide face (a) and narrow face corner(b)

3.3 New formation mechanism for shell hot spots

Fig. 5 shows the evolutions of the shell surface temperatures and the thermal resistances of mold flux and air gap around the wide and narrow face corners at various distances below meniscus. Because the generation of the mold/solid flux interfacial contact thermal resistance results from the mold flux film solidification shrinkage and deformation, the thermal resistance in this study was considered as a part of the mold flux thermal resistance. Thus, the mold flux thermal resistance in the figures consists both that of mold flux film and the mold/solid flux interfacial contact thermal resistance.

For the wide face, in accordance of the distribution characteristic of mold flux film in the gap, its thermal resistance also distributes first increase and then decrease from the corner to the midst in the mold, and therefore the peak value of the thermal resistance appears in the off-corner during the casting, as shown in Fig. 5(a). As the result of the mold flux thermal resistance such distribution characteristic, the shell off-corner heat transfer is greatly slowed down, and the hot spot gradually forms accordingly that the obvious higher shell surface temperature generates with a expanding temperature difference between the off-corner and the midst at the positions of 200–700mm below meniscus. During this process, although the air gap forms with a much greater thermal resistance around the corner, it is not the cause of giving rise to the shell off-corner form the hot spot due to the air gap formation region is too close to the corner that the two dimensional heat transfers of the corner counteract the temperature increase. When the shell moves down below 700mm from meniscus, the thick air gap spreads to the direction of the shell midst that the much greater thermal resistance reduces the heat transfer of the shell where closer to the corner more greatly, and a new and much serious hot spot forms at the mold exit. Hence, at the upper and middle parts of mold, the formation of shell wide face off-corner hot spot results from the thick mold flux film filling in the shell/mold gap, while it results from the thick air gap formation near to the mold exit.

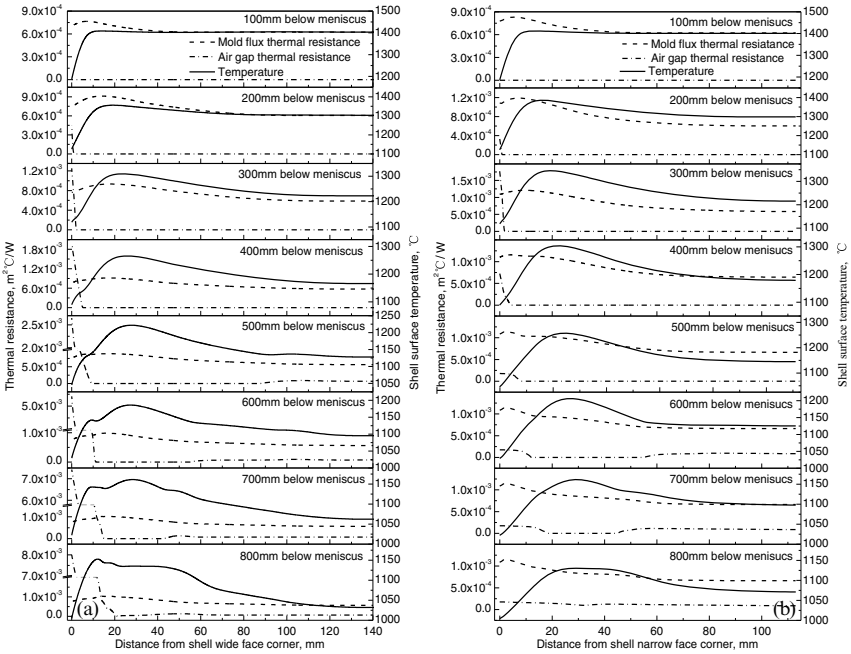

Fig. 5 The evolutions of mold flux and air gap thermal resistances in shell/mold gap and shell surface temperature around shell wide face corner (a) and narrow face corner (b)

As for the narrow face, as shown in Fig. 5(b), the off-corner hot spot formation mechanism has some differences. Since the air gap formation in shell narrow face is much closer to the corner that it just concentrates in the region of 0–10mm from the corner with thinner thickness, as seen from Fig. 4(b), the air gap does not have any effect on the shell off-corner heat transfer during the whole solidification process of shell in mold. Therefore, the formation of the hot spots in shell narrow face just results from the thick mold flux film filling in the shell/mold gap in the off-corner. Furthermore, since the maximum thickness difference of the mold flux film between the shell off-corner and the midst appears at 300mm below meniscus, the most serious hot spot forms at the position accordingly. It is rather different from the previous formation mechanism that considered the hot spots formation in shell wide and narrow face off-corners in the mold resulting from the air gap formation.

Conclusions

(1) Under the typical slab casting conditions of carbon steel, the thick mold flux film concentrates in 0–120mm and 0–70mm off the shell wide and narrow face corners, and the air gap first forms in shell corner and mainly concentrates in 0–20mm and 0–10mm off the corners in mold. The mold flux films around the wide and narrow face off-corners distribute first

increase and then decrease from the corner to the midst. The maximum thickness on shell wide face is 1.01mm at the mold exit, while on the narrow face is 1.27mm at 300mm below meniscus. The air gap on shell wide face grows continuously and increases at 550mm below meniscus, where it mainly forms in 160–450mm below meniscus on shell narrow face. The maximum thickness on shell wide face is 0.8mm at the mold exit, while on the narrow face is 0.17mm at 300mm below meniscus.

(2) Under the typical slab casting conditions of carbon steel, the hot spots form in the regions of 10–80mm and 15–60mm off the shell wide and narrow face corners with an expanding trend with shell moving down. The maximum temperature differences between the off-corners and the corresponding midst reach 120 ºC at mold exit and 129 ºC at 300mm below meniscus.

(3) The formation for shell wide face off-corner hot spot results from the thick mold flux film filling in the shell/mold gap at the mold upper and middle parts, while the lower part results from the thick air gap formation, and that of the narrow face just results from the thick mold flux film filling in the gap in the off-corner.

Acknowledgement

The National Natural Science Foundation of China (51404061) is acknowledged for supporting this work.

References

[1] J.K. Brimacombe, Metall. Mater. Trans. 24B (1993) 917-935.
[2] B.G. Thomas, W.R. Storkman, Modeling Casting Welding Proc. (1988) 287-297.
[3] B.G. Thomas, A. Moitra, R. McDavid, Iron Steelmaker 23 (1996) 57-70.
[4] Z.Z. Cai, W.L. Wang, M.Y. Zhu, Mater. Sci. Technol. Int. Conf. (2012) 61-72.
[5] A. Grill, K. Sorimachi, J.K. Brimacombe, Metall. Mater. Trans. 7B (1976) 177-189.
[6] J.O. Kristiansson, J. Thermal Stresses 7 (1984) 209-226.
[7] E.G. Wang, J.C. He, Z.K. Yang, H.G. Chen, Iron Steel 34 (1999) 25-27.
[8] E.G. Wang, J.C. He, Sci. Tech. Adv. Mater. 2 (2001) 257-263.
[9] K. Kim, H.N. Han, T. Yeo, Y. Lee, K.H. Oh, D.N. Lee, Ironmaking Steelmaking 24 (1997) 249-256.
[10] H.N. Han, J.E. Lee, T.J. Yeo, Y.M. Won, K.H. Kim, K.H. Oh, J.K. Yoon, ISIJ Int. 39 (1999) 445-454.
[11] Y. Meng, B.G. Thomas, Metall. Mater. Trans. 34B (2003) 685-704.
[12] C. Li, B.G. Thomas, Metall. Mater. Trans. 35B (2004) 1151-1172.
[13] S. Ozawa, M. Susa, T. Goto, R. Endo, K.C. Mills, ISIJ Int. 46 (2006) 413-419.
[14] R. Saraswat, D. M. Maijer, P. D. Lee, K. C. Mills, ISIJ Int. 47 (2007) 95-104.
[15] H. Nakada, M. Susa, Y. Seko, M. Nayashi, K. Nagata, ISIJ Int. 48 (2008) 446-453.
[16] K.C. Mills, A.B. Fox, ISIJ Int. 43 (2003) 1479-1486.
[17] Z.Z. Cai, M.Y. Zhu, Acta Metall. Sin. 47 (2011) 678-687.
[18] Z.Z. Cai, M.Y. Zhu, Acta Metall. Sin. 47 (2011) 671-677.
[19] K. Watanabe, M. Suzuki, K. Murakami, H. Kondo, A. Miyamoto, T. Shiomi, Tetsu-to-Hagané 83 (1997) 115-120.
[20] J.W. Cho, H. Shibata, T. Emi, M. Suzuki, ISIJ Int. 38 (1998) 440-446.
[21] J.W. Cho T. Emi, H. Shibata, M. Suzuki, ISIJ Int. 38 (1998) 834-842.
[22] Z.Z. Cai, M.Y. Zhu, Acta Metall. Sin. 45 (2009) 949-955.